## 1 Samples of garment sewing pattern

We show garment sewing pattern samples in Fig.9, including a dress, pants, a shirt, and a skirt. Since sewing patterns offer common information about the garments, they are generally available.

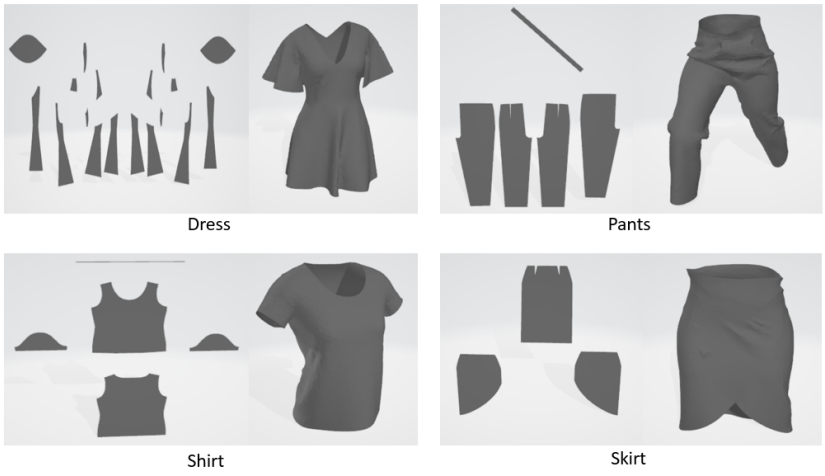


**Fig. 9.** Garment sewing pattern samples. We show 4 cases here, including a dress, pants, a shirt, and a skirt. Since sewing patterns offer common information about the garments, they are generally available.

## 2 Example Meshes from Our Garment Dataset

In Fig. 10, we show that our garment dataset consists of clothing on different human body poses/sizes/shapes and of varying garment topologies, patterns, and materials. We sample ten human motions from the CMU MoCap dataset, including motions of walking, running, climbing and dancing. As stated in the main text, we have over 100 different garment types in the dataset, including dresses, t-shirts, pants, skirts and swimsuits. We use different material parameters and material space scales to control the sizes of the garments. Given this large and diverse dataset, our network can successfully disentangle different parts of the body label to generate garments with topologies totally different with those in the training dataset, while keeping a visually plausible result.

## 3 One-hot Version of the Label Image

In Fig. 2, we first transfer the label image to one-hot version by the one-hot operation. One-hot version of the label image is an array of binary images, where each pixel

**Fig. 10.** Examples meshes from our garment dataset. The dataset includes several common garment topologies and materials, as well as various human poses. The last two columns show the same garment pattern with different materials. The wrinkle appearances of the two sequences are different.

on the i-th binary image represents whether the label ID of that pixel on the original image equals to i. We use one-hot to support different garment components (e.g., shirts+jacket+pants) in future work. One-hot version of label image can decouple different class IDs and will be easier for the network to learn. Currently, we use it to differentiate between garment and other pixels. Overall, it is an extensible data format.

## 4 Data Format Transfer Process

Fig. 11 shows the data format transfer process. The garment model and the image representation of the garment can transfer to each other using the body mesh and UV map, as discussed in Sec. 4.

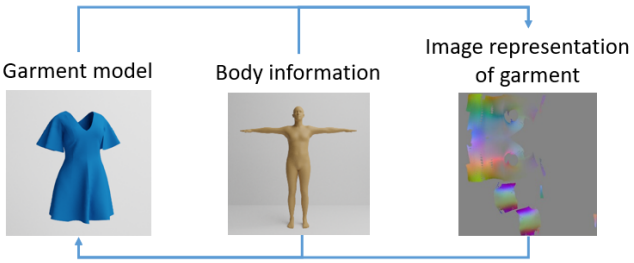


**Fig. 11.** Data format transfer process. The garment model and the image representation of the garment can transfer to each other using the body mesh.

## 5 Point Matching between Body and Garment

We show the mapping process from body surface pixels to the garment surface in Fig. 12. Within the Voronoi region of a body vertex, the ray direction of a pixel (brown) is interpolated between the vertex normal (black) and the face normal (gray), according to the barycentric coordinates.

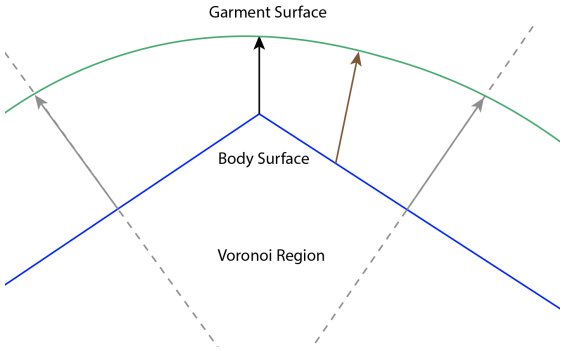


**Fig. 12.** Mapping from body surface pixels to the garment surface. Within the Voronoi region of a body vertex, the ray direction of a pixel (brown) is interpolated between the vertex normal (black) and the face normal (gray), according to the barycentric coordinates.

## 6 Reconstruction Results under Different Conditions

We show in Fig. 14 that our algorithm introduced in Sec. 4 is robust to any kind of garment input. We tested our algorithm with garments of different topologies on different human bodies. Different cloth materials are expressed with different sizes and detailed

wrinkles based on the geometry. Our method can also retain the material information faithfully.

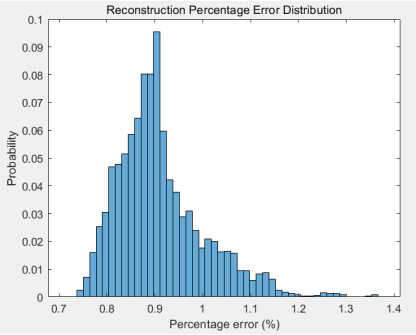


**Fig. 13.** Distribution of reconstruction error $d_m$ (in percentage w.r.t. the garment height) over $6,000$ randomly selected garment instances. The error is relatively small across all types of garments, with the largest being less than $1.4\%$ and most within $1\%$.

Fig. 13 shows the distribution of $d_m$ in our training dataset. The error is relatively small across all types of garments, with the largest being less than $1.4\%$ and most of them within $1\%$.

## 7 Garment Retargeting

In Sec. 6.5, we show the garment retargeting results using only a T-pose. In Fig. 15, we show more cases with different poses. As shown in the figure, our method can retarget garments with different topologies, patterns, and materials to bodies with different shapes, sizes, and poses.

## 8 Performance

Our method takes about 2,248 msec on average. For garment generation, 2 seconds would be quite acceptable if the quality is good enough, while the garments designed manually usually take much longer. Also, there is room for performance improvement and parallelization of the post-processing after the network inference. More importantly, we use a resolution of 512*512 for the displacement map, so there are up to 512*512 vertices and 511*511*3 edges in our reconstructed mesh, with resolution much higher than other works, thus taking slightly longer. As needed, the implementation of our method can be much improved by reducing the resolution of the displacement map.


**Fig. 14.** Reconstructed mesh results under different human poses and shapes, garment topologies, sizes, and materials. Our data transfer method is able to map any 3D mesh to its 2D image representation with little information loss.

**Fig. 15.** Garment retargeting results. Our method can retarget garments with different topologies, patterns, and materials to bodies with different shapes, sizes, and poses.